ELSEVIER

Nuclear Instruments and Methods in Physics Research A 432 (1999) 342–357

NUCLEAR INSTRUMENTS & METHODS IN PHYSICS RESEARCH Section A

www.elsevier.nl/locate/nima

Analysis of radiation effects on silicon strip detectors in the NA50 experiment

B. Alessandro[a], S. Beolé[a], G. Bonazzola[a], E. Crescio[a], W. Dąbrowski[b], P. Giubellino[a], P. Grybos[b], M. Idzik[a,b,*], M. Martinetto[a], A. Marzari-Chiesa[a], M. Masera[a], F. Prino[a], L. Ramello[a], P. Rato Mendes[a], L. Riccati[a], M. Sitta[a]

[a]*INFN, Via P. Giuria 1, 10125 Torino, Italy*
[b]*Faculty of Physics and Nuclear Techniques, UMM, Cracow, Poland*

Received 22 January 1999

Abstract

During the operation of the Multiplicity Detector in the NA50 experiment the single sided AC-coupled *p-on-n* silicon strip detectors were exposed to charged particle fluences resulting in an equivalent 1 MeV neutron fluence up to 10^{14} eq. n/cm^2 and a total ionising dose up to 20 Mrad, with a very non-uniform radiation spatial distribution. In this paper detailed analysis of radiation effects observed on the detectors during the 1996 lead ion run as well as results of measurements performed after the run are presented.

1. Introduction

The Multiplicity Detector of the NA50 experiment [1] is one of very few detectors working in a real experiment where silicon detectors were exposed to radiation fluences and doses comparable to the ones expected for the LHC inner trackers [2]. Therefore, radiation resistance of this detector is of great interest from the point of view of the LHC experiments as well as the NA50 experiment. Here we present the final results of the analysis on radiation effects observed during two years of operation of our detector. Preliminary results can be found in Ref. [3].

In this paper we first briefly describe the silicon multiplicity detector in the NA50 experiment, with particular attention to the expected effects of radiation. Next we discuss the methods to monitor radiation damage effects during data taking, together with results obtained during the 1996 ion run. Afterwards we present the results of the measurements performed after the run in order to cross-check the observations from the data taking period and to better understand the behaviour of the detectors after type inversion.

2. The Multiplicity Detector in the NA50 experiment

NA50 is a fixed target experiment investigating the production of resonances decaying to dimuons produced in high-energy (158 A GeV/*c*) PbPb

* Corresponding author. INFN Torino, via P. Giuria 1, 10125 Torino, Italy.

0168-9002/99/$ - see front matter
PII: S0168-9002(99)00462-3

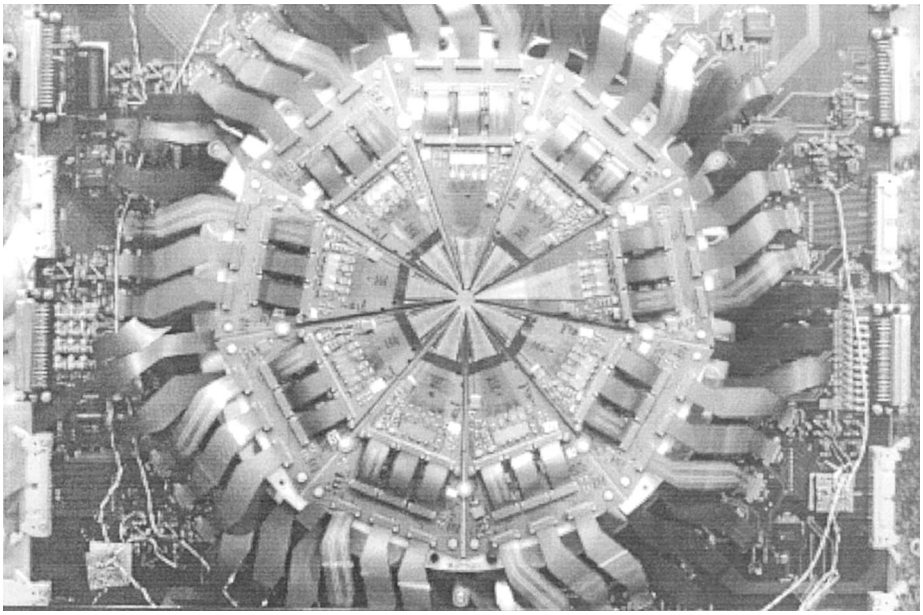

Fig. 1. View of the single plane of the multiplicity detector.

interactions at the CERN SPS. The silicon microstrip detectors are used in the NA50 experiment for charged multiplicity measurements and for target recognition.

The layout of the NA50 experiment imposed several important constraints on the design of the silicon multiplicity detector. Given the high interaction rate, a very short deadtime of the readout electronics (< 50 ns) was implemented. The radial microstrip detectors were designed with a constant segmentation in pseudorapidity ($\Delta\eta = 0.02$) and in the azimuthal angle ($\Delta\phi = 10^0$). The view of one of the two planes of the multiplicity detector is shown in Fig. 1. Both of them are positioned centrally behind the target. The primary beam crosses the hole visible in the middle of the photograph. A single detector unit is shown in Fig. 2. It consists of 2×128 AC-coupled *p-on-n* strips with a pitch ranging from 90 μm at the tip of the detector to 700 μm in the outermost part. In this paper we refer to the innermost strip as to the strip number 1 and number the strips successively up to strip 128 for the outermost one. The design of the detector implies constant occupancy per readout channel while the number of particles per unit area, and therefore the radiation dose, has a highly non-uniform radial distribution, decreasing rapidly with increasing radius. In Figs. 3 and 4 we show the results of the Monte Carlo simulation of the expected fluences and doses for the 1996 ion run. In the simulation, the detectors are assumed to be perfectly symmetric with respect to the beam axis, while in reality there

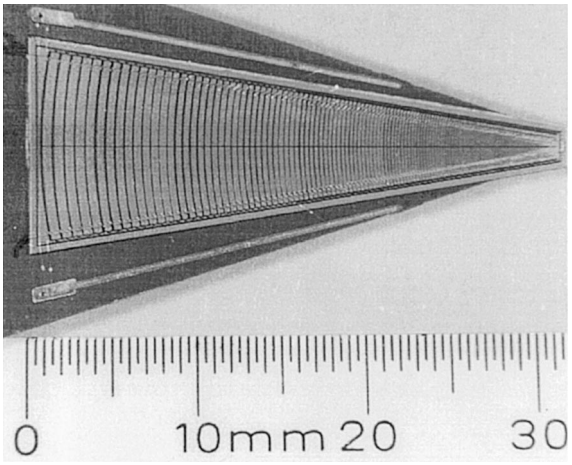

Fig. 2. View of one of the AC-coupled single detector units.

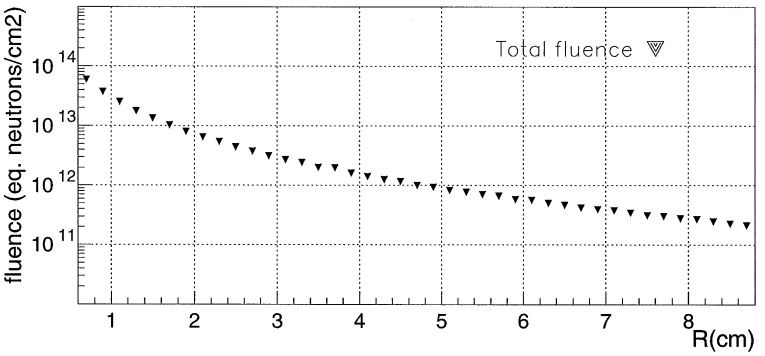

Fig. 3. The Monte Carlo simulation of the received fluence during the 1996 ion run.

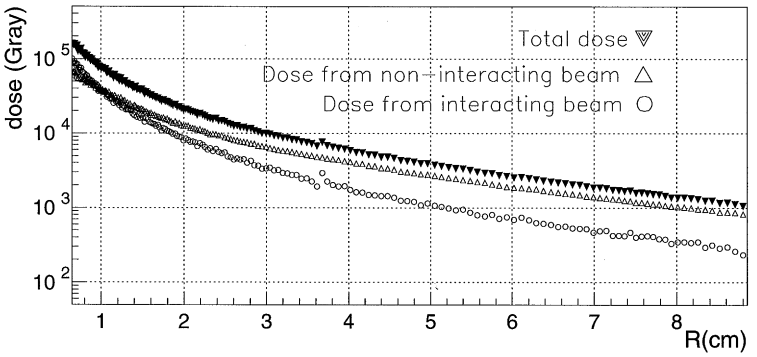

Fig. 4. The Monte Carlo simulation of the received dose during the 1996 ion run.

was a shift of several hundred microns from the nominal position. Therefore, given the strong radial dependence of the radiation distribution, the innermost strips of some of the detectors received considerably more radiation than the simulated value.

The dominant component of the displacement damage is generated by the particles produced in the PbPb interactions, with a minor component of backsplash from the hadron dump and the calorimeters. The total ionizing dose has two significant components with slightly different angular distributions, as shown in Fig. 4: the particles produced in the PbPb interactions and the delta rays (knock on electrons) copiously produced by the high field of the Pb nucleus while crossing the target without undergoing a nuclear collision. For the innermost part of the detector the simulated fluence reaches almost 10^{14} eq. n/cm^2, corresponding to a flux value of about 2.5×10^8 eq. n/(s cm^2), and 20 Mrads of ionising dose, corresponding to a dose rate 50 rad/s. Therefore, from the present knowledge of radiation damage to silicon due to charged particles, one should expect for most of the detectors the substrate to be transformed from n-type to p-type after the 1996 ion run.

In the following we will report on radiation effects observed during the 1996 lead ion run. We should mention here that 5/6 of the detectors had also been used during a previous lead run in 1995, when they received roughly 1/4 of the 1996 run radiation. In considering the effects of the 1995 radiation one should include the fact that the detectors were left to anneal at room temperature for one year.

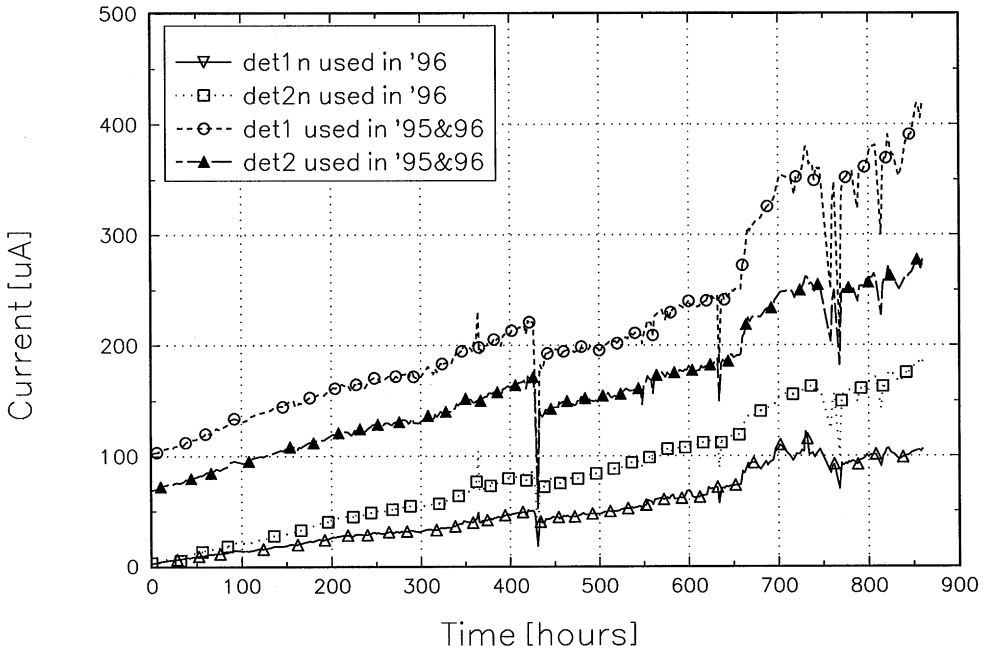

Fig. 5. Typical leakage currents of individual detectors during the 1996 ion run.

3. Radiation effects observed during the 1996 lead run

Immediate radiation damage effects were observed during the data taking period: increase of the leakage currents and change of the depletion voltages which, after type inversion, started to increase and eventually passed the standard setting of 60 V. The leakage current in each detector (256 strips) was measured directly, by monitoring the multichannel power supply, whereas there was no direct way to measure the depletion voltage during data taking. An observable correlated to the thickness of the depletion layer, and which therefore can provide information on the depletion voltage, is the occupancy of particles measured in the detector, i.e. the average fraction of events for which the signal is higher than the applied threshold. In the following we discuss the radiation effects observed during the run on the basis of leakage currents and occupancy measured in the detector.

3.1. The leakage current

The leakage currents of the detectors were monitored continuously during the run. In Fig. 5 the leakage currents for detectors irradiated during the 1996 and during both the 1995 and 1996 ion runs are shown. The plotted values of these currents are taken at the working temperature of the detectors, which is considerably higher than the ambient temperature in the experimental area (23°) due to heating by the frontend electronics. From the measurements of the leakage currents at ambient temperature, with the frontend electronics switched OFF, and at working temperature we estimate the average working temperature to be $35° \pm 2°$. The few sharp changes of the current visible in Fig. 5 are linked to changes in the cooling system, power supply breakdowns, periods of interruption of the run, and bias voltage changes. Under the realistic assumption of almost constant average beam intensity, the currents scale linearly with the received fluence, in agreement with the

phenomenology. The leakage current shown in Fig. 5 is the total current of a detector, comprising strips irradiated up to fluences varying by more than one order of magnitude between the innermost and the outermost ones. Therefore, the damage constant resulting from these measurements is not directly comparable to values obtained by other radiation tests, like e.g. [4]. Yet, it is well known that the leakage current of an irradiated diode is proportional to its area, assuming a constant thickness, multiplied by the fluence (assumed constant over its area) of equivalent neutrons received. In our case, given the different size of the strips, the number of impinging particles per strip is approximately constant (all strips had roughly the same counting rate), and so they all have approximately the same product of received fluence times area. Thus, to a first approximation, all strips have the same leakage current, equal to the total detector current divided by the number of strips. At the end of the 1996 ion run the average current per strip was around 1 μA (detectors irradiated in 1996 only). Thanks to a short integration time of our frontend electronics, these fairly large currents affected only marginally the operation of the readout electronics, resulting only in a modest increase of the total noise. The signal-to-noise ratio remained almost unchanged at the level of ~ 15 [1].

3.2. Breakdown voltage

In the design of the silicon multiplicity detector no special features assuring high voltage operation were employed. Nevertheless, no detector breakdown was observed during the 1996 ion run. Fig. 6 shows some of the I–V characteristics measured at the end of the 1996 run by varying the detector bias voltage (HV scan). At this stage all detectors were already inverted and no sign of breakdown was visible. All the strips in a single detector were biased at the same voltage, although the actual full depletion voltage varied from ~ 20 V, for the outermost strips, to ~ 200 V for the inner ones. All of the 36 non-uniformly irradiated detectors were working successfully after type inversion, with applied bias voltage up to at least 180 V. During the tests

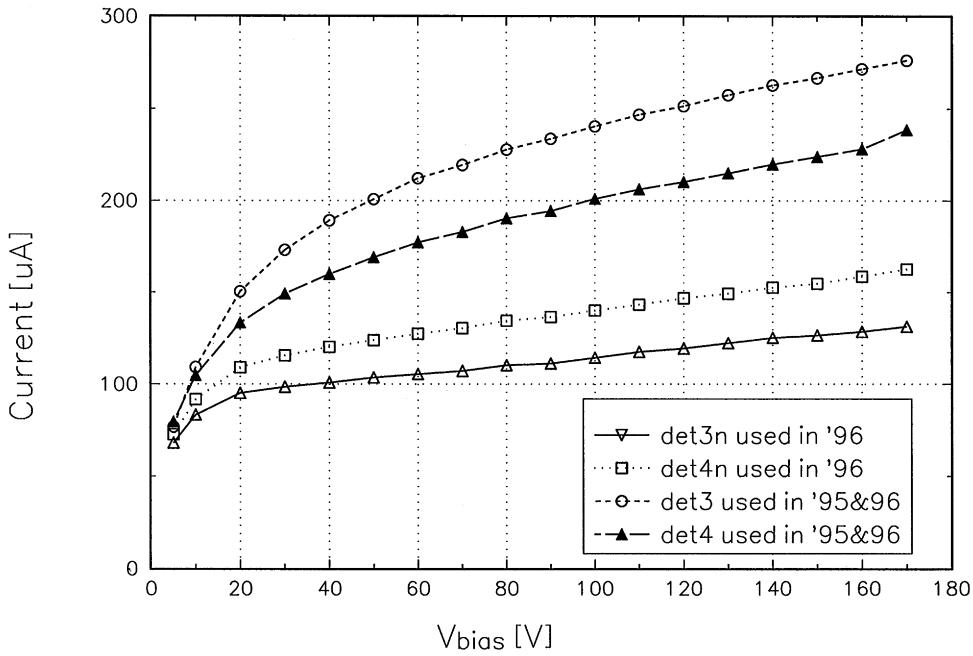

Fig. 6. The leakage currents vs. bias voltage at the end of the 1996 ion run.

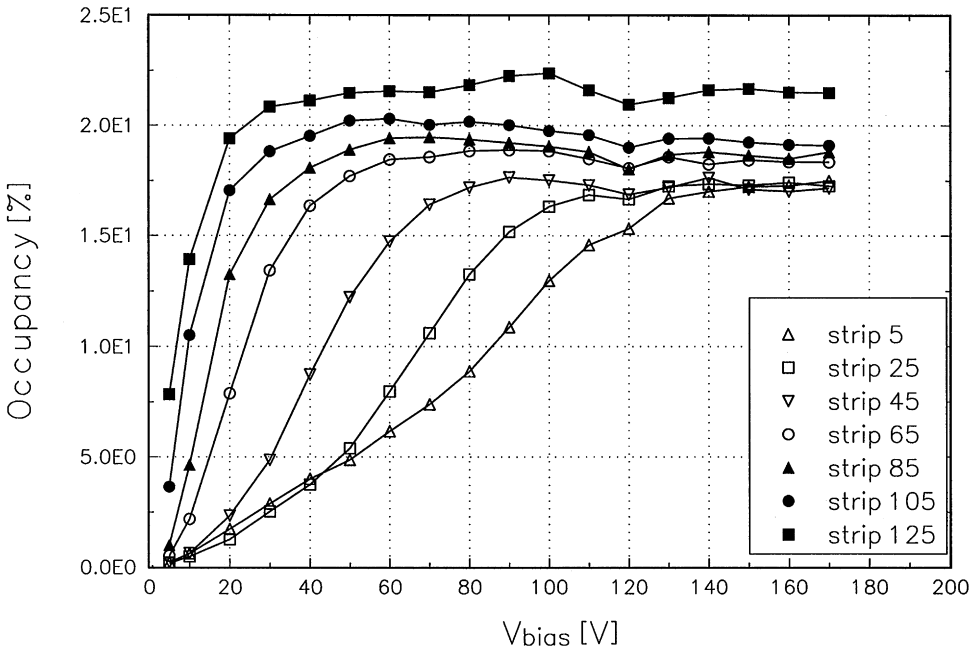

Fig. 7. Strip occupancy vs. bias voltage at the end of the 1996 ion run for detectors used only in the 1996 run.

after the run bias voltages between 200 and 400 V were applied to some of the detectors and none of them became unusable. Our observations confirm the effect of increasing breakdown voltage of *p-on-n* detectors after type inversion, as observed in other radiation experiments [5].

3.3. Occupancy vs. detector bias voltage

At the end of the 1996 ion run we performed detector bias voltage scans while taking data in order to measure the effects of the irradiation on the detectors. Figs. 7 and 8 show typical curves of the occupancy vs. detector bias voltage for detectors used in the 1996 ion run and in both the 1995 and 1996 ion. One can see that the occupancy for the innermost strips of detectors used in 1995 and 1996 does not saturate for the highest applied bias voltage. In order to correlate the depletion voltage to measured occupancy as a first approximation, we assumed that occupancy $\sim Q_{\text{collected}} \sim W_{\text{depleted}} \sim \sqrt{(V_{\text{bias}})}$. Using a simple algorithm which finds the crossing point of two linear fits the depletion voltage was evaluated strip by strip (Fig. 9) on the basis of the occupancies obtained during the HV scans. In the same figure the depletion voltages measured for one of the detectors just after the 1996 ion run with the standard C–V method are presented. The depletion voltages calculated from the strip occupancy are in reasonable agreement with the ones obtained from C–V measurements. Bias voltage scans appear to be a very powerful method allowing to get in one measurement information about the depletion voltage individually for each strip. From the data shown in Figs. 7 and 8 it is clear that the depletion voltages of the innermost strips of detectors used during both the 1995 and the 1996 runs exceed the limit of our power supply which was 200 V during the 1996 run. Since these detectors were kept at room temperature between the 1995 and the 1996 ion runs, one should expect that significant reverse annealing took place [6]. Indeed, although the total fluence in the 1995 run was about 1/4 of the 1996 run, the depletion voltages for these detectors were

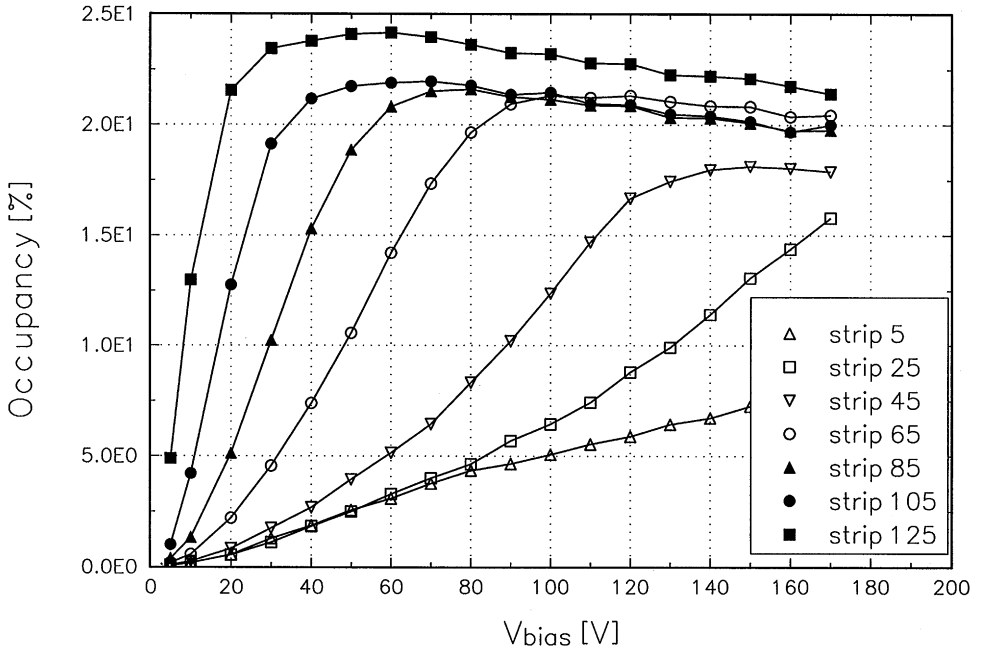

Fig. 8. Strip occupancy vs. bias voltage at the end of the 1996 ion run for detectors used in both the 1995 and the 1996 runs.

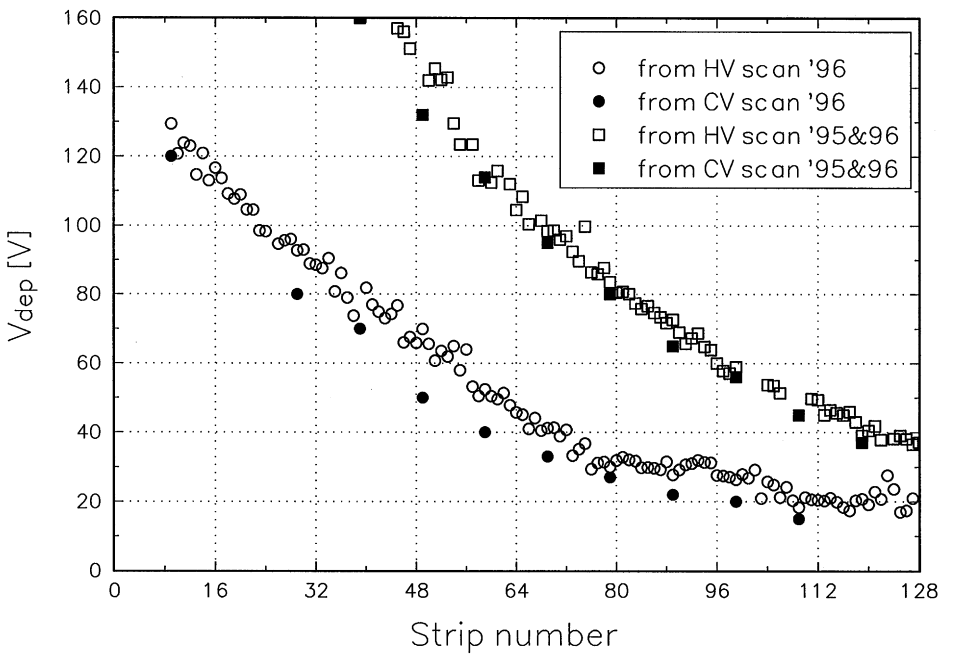

Fig. 9. Strip by strip depletion voltages calculated from the occupancies measured in the HV scan and obtained from *C–V* measurements.

more than double of the ones used only in the 1996 run. It is known that the depletion voltage decreases with radiation until the type inversion, where its value is close to zero, and then it grows with received fluence. We observed (Fig. 9) that the depletion voltage increases with fluence, confirming that the detectors have undergone type inversion.

3.4. Detector efficiency

In order to evaluate the efficiency of irradiated detectors we compared the saturation value of the strip occupancy (shown in Fig. 7) with the physical occupancy of the particles, obtained from the counting rate measured at the beginning of the run, when the detectors were not yet irradiated. For strips which were fully depleted, no decrease of the efficiency (within the accuracy of 10%) was observed. Obviously, for strips which were not fully depleted we observed a significant drop of efficiency. We can, however, conclude that standard *p-on-n* detectors operate successfully at fluences up to 10^{14} eq. n/cm^2 and do not show significant loss of efficiency provided they are biased at high enough voltage to be fully depleted.

3.5. Interstrip isolation after type inversion

After the 1996 ion run we performed a test exposing the detectors directly to the primary SPS proton beam (450 GeV/c) in order to investigate the isolation of p + strips after type inversion in the detector. Fig. 10 shows the ratio of double strip clusters to the total number of clusters, measured for different bias of the detector (from the HV scans we know that approximately 100 V was enough to deplete the strips above the strip number 70 while 200 V depleted the ones above the strip number 30). Due to the limited statistics, the measured data are accurate to about 30%. Given the low beam rate and the negligible crosstalk, double strip clusters, i.e. pairs of contiguous hit strips, can be attributed to sharing of the charge among them. In Fig. 10 we show also the values simulated with GEANT under the hypothesis of different widths of the charge sharing region in the detector. In all cases the

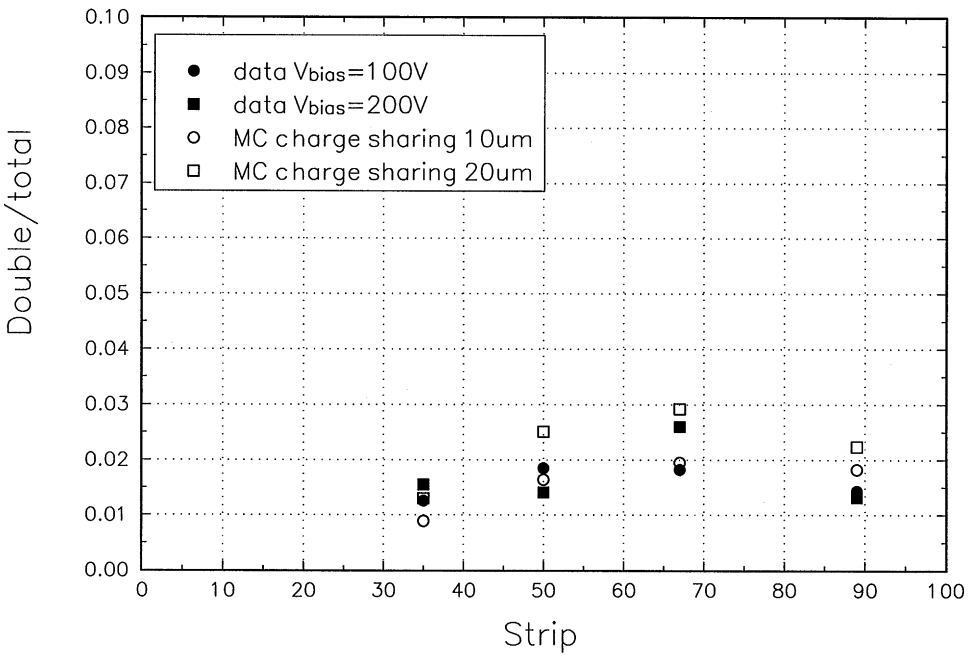

Fig. 10. Ratio of the number of double strip clusters to single strip ones obtained with proton beam and simulated with GEANT.

measured fraction of double strip clusters is of the order of 2% in good agreement with the Monte Carlo simulation and is not significant in absolute terms. We can conclude that no evidence of lack of isolation between strips of the inverted detector was observed, even for the strips which were not fully depleted.

4. Post-run measurements

In order to cross-check the observation of radiation effects performed during the run, as well as to investigate in detail the behaviour of inverted detectors, a set of laboratory measurements was performed after the 1996 ion run for some of the detectors. We concentrated on standard detector electrical parameters performing AC impedance measurements, using the HP4284A variable frequency LCR meter, and DC I–V measurements. Keeping in mind that radiation induced effects are characterized by relatively long time constants, we devoted particular attention to the frequency dependence of the measured quantities. We should remind that because of the very non-uniform irradiation each detector unit represents a sample of strips with depletion voltages ranging from few tens to few hundreds of volts. In the following we present a selection of typical results concerning capacitance to the backplane, interstrip capacitance and AC and DC interstrip resistance. We also discuss the behaviour of the p+ side after type inversion.

4.1. Capacitance to the backplane

Before irradiation the capacitance to the backplane C_{back} was measured and no frequency dependence was observed. On the contrary, we have observed a significant frequency dependence, varying with the applied bias voltage, for the detectors used in the 1995 and 1996 ion runs, which underwent type inversion. Figs. 11 and 12 show typical curves of $1/C^2_{\mathrm{back}}$ vs. bias voltage for inverted strips, measured for the oscillator frequency range 10–200 kHz.

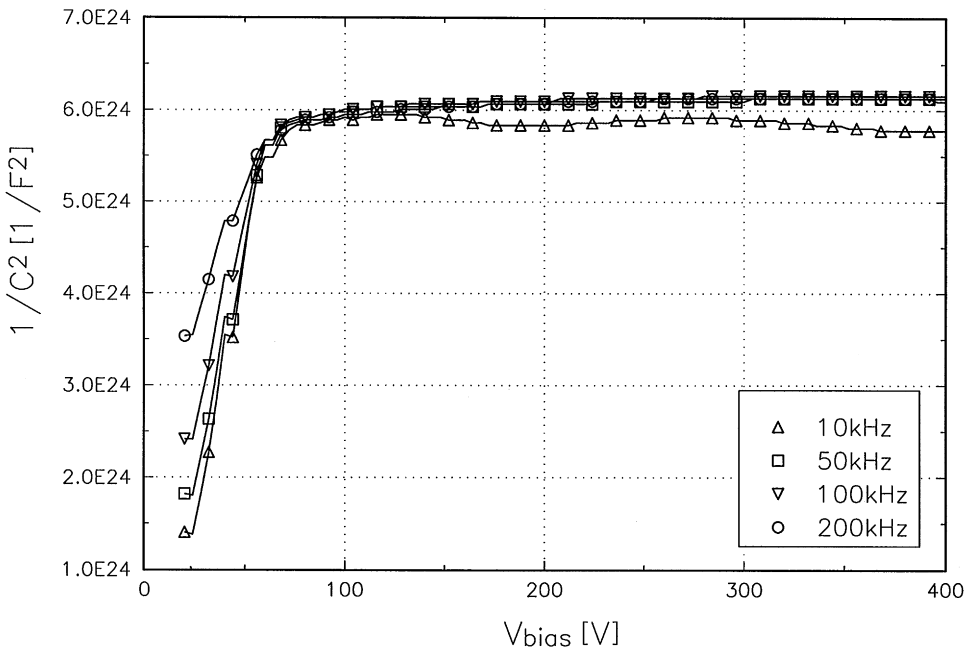

Fig. 11. $1/C^2_{\mathrm{back}}$ vs. bias voltage for strip number 100.

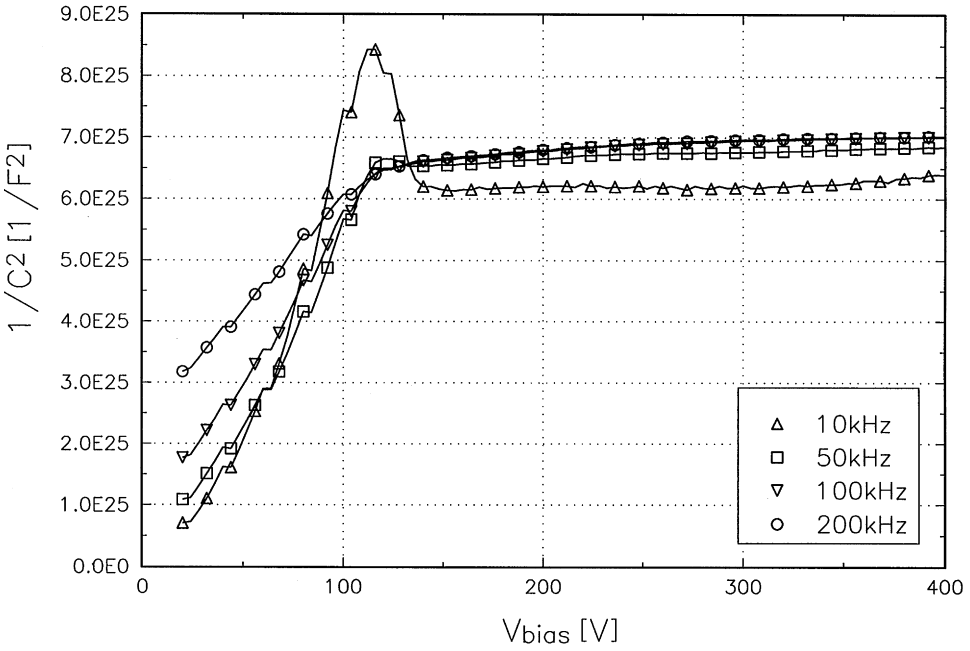

Fig. 12. $1/C^2_{back}$ vs. bias voltage for strip number 60.

One can see that the $1/C^2$ method allows to evaluate the full depletion voltage in this frequency range. Measurements for frequencies below 10 kHz and above 200 kHz were done as well but the shapes of the curves were more complex and did not allow simple linear fits. As it was mentioned before, the depletion voltages estimated in this way agree with the ones obtained from the occupancy in the HV scan performed at the end of the 1996 run (see Fig. 9). Figs. 13 and 14 show C_{back} vs. oscillator frequency, measured for bias voltages, respectively below and above the depletion voltage. The capacitance vs. frequency characteristics for the bias voltages below the full depletion voltage show typical shapes indicating the presence of deep energy levels in the band gap [7]. Two dominant radiation induced levels are observed, at ~ 500 Hz and at ~ 100 kHz. For bias voltage above full depletion the latter one practically disappears. The frequency dependence of C_{back} vanishes for $V_{bias} \sim 400$ V, which is much higher than $V_{dep} \sim 40$ V, and C_{back} recovers its purely geometrical value.

4.2. Interstrip capacitance

Before irradiation no frequency dependence of the interstrip capacitance C_{int} was observed. In Fig. 15 typical curves of C_{int} vs. bias voltage for an inverted detector are shown. All curves converge to the same, purely geometrical value for a very high bias voltage which is, similarly to what was observed for C_{back}, several times higher than the depletion voltage. Measurements of C_{int} vs. oscillator frequency for different bias voltages are shown in Fig. 16. Unless a very high bias voltage is applied, all curves show a similar behaviour with a smooth raise up to 5–50 kHz and then a very slow fall. The frequency dependence of C_{int} at voltages above the depletion voltage may result from the electron surface layer in the interstrip region. In order to remove this layer and to recover the geometrical value of the capacitance, a detector bias voltage much higher than the depletion voltage may be required.

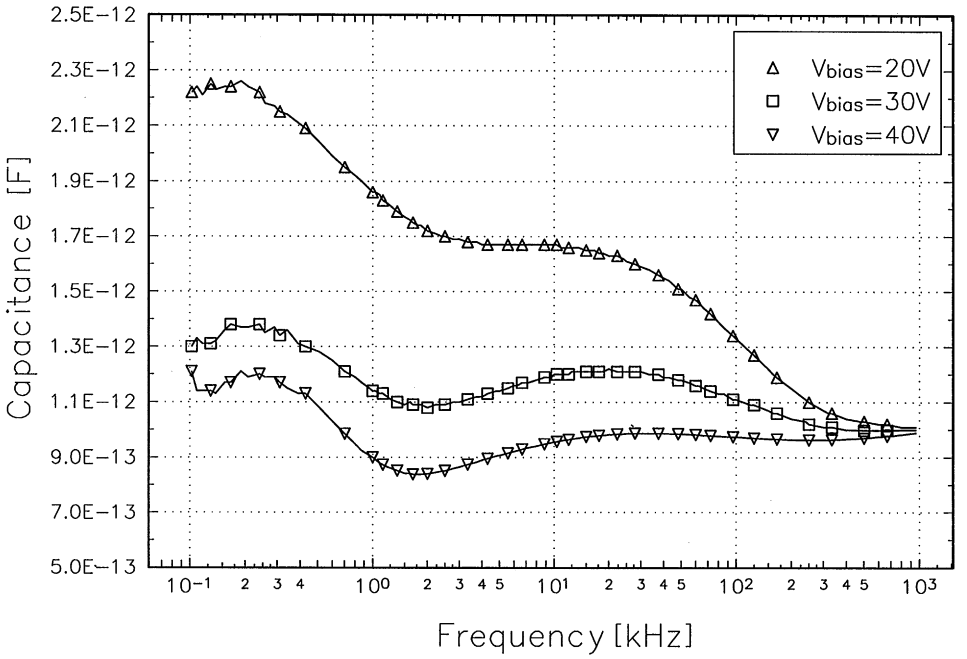

Fig. 13. C_{back} vs. frequency for strip 115 for 3 bias voltages, all below full depletion.

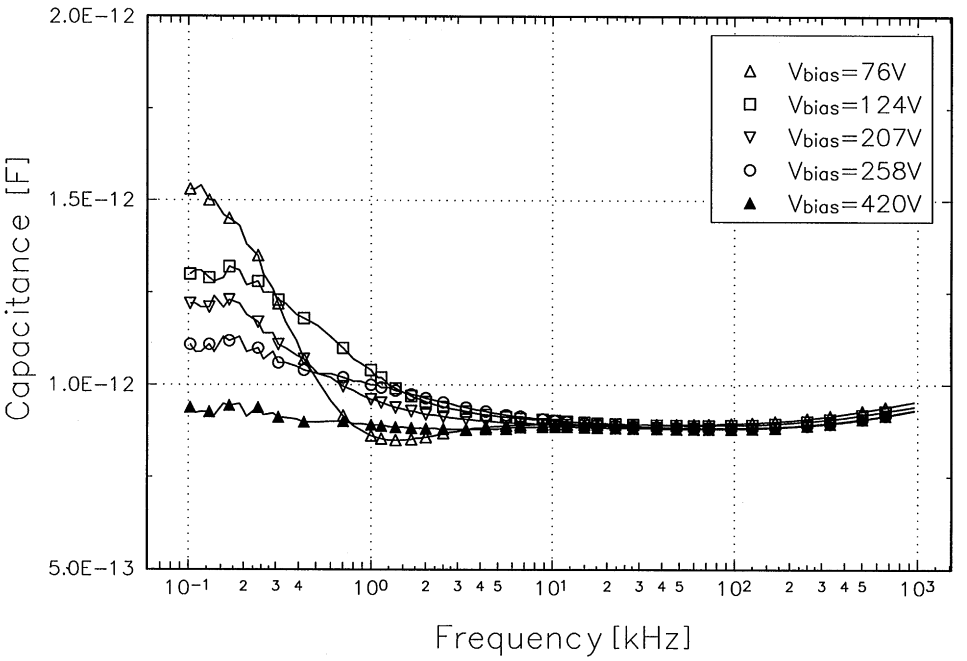

Fig. 14. C_{back} vs. frequency for strip 115 for 5 bias voltages, all above full depletion.

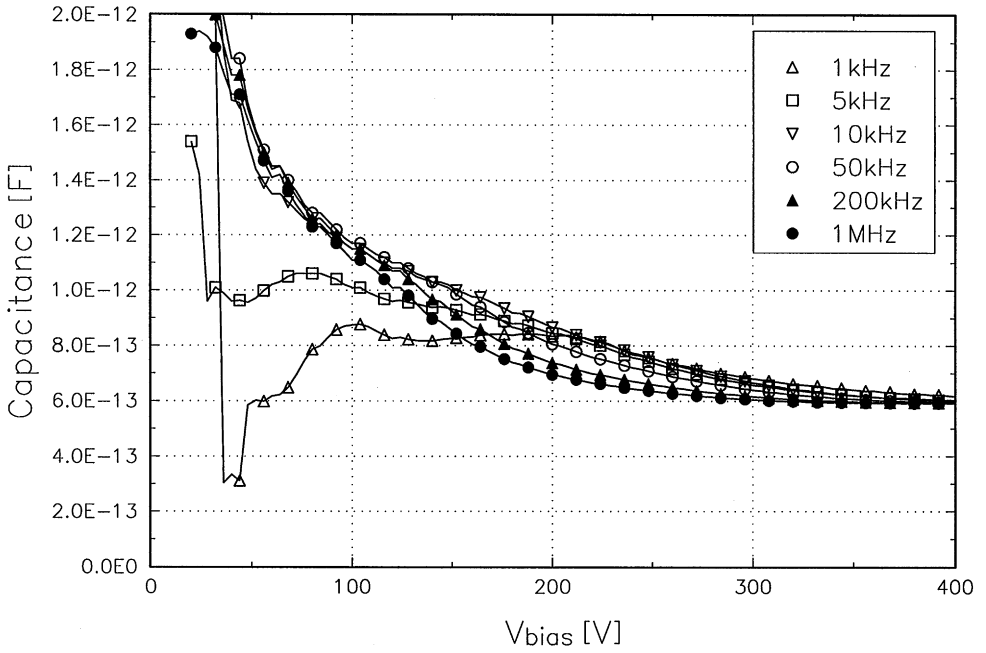

Fig. 15. C_{int} vs. bias voltage for strip 115, which has $V_{\text{dep}} = 40$ V.

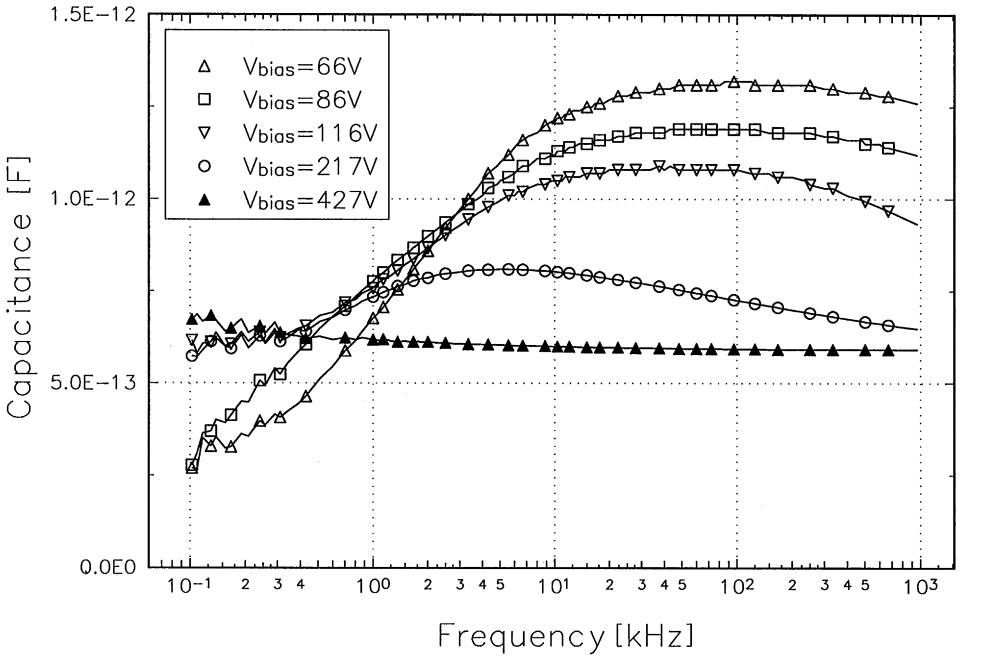

Fig. 16. C_{int} vs. osc. frequency for strip 115 with $V_{\text{dep}} = 40$ V.

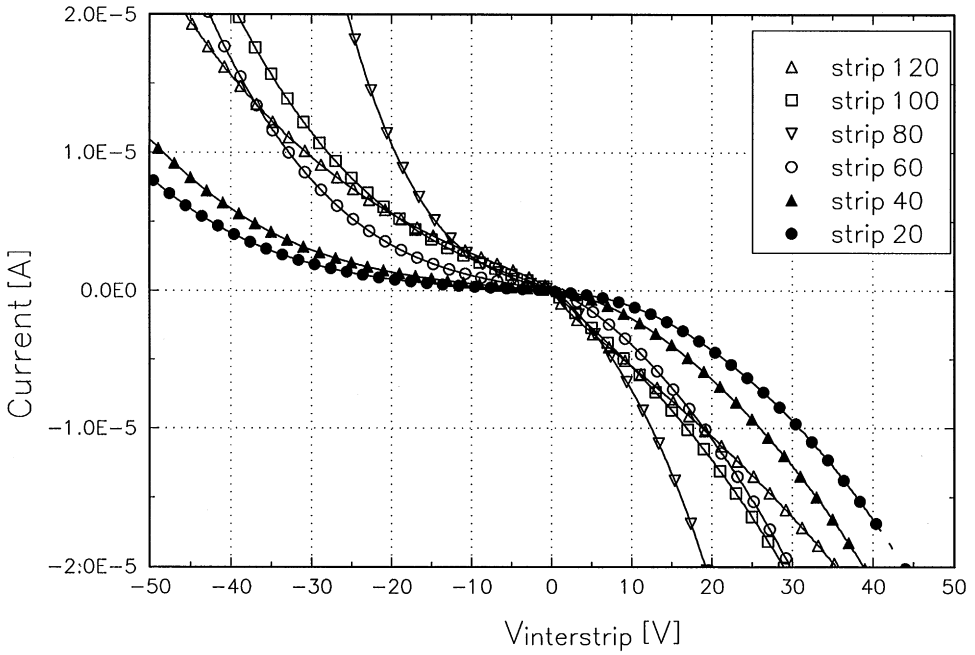

Fig. 17. Interstrip I–V curves for different strips measured with floating detector backplane.

4.3. Interstrip resistance

In order to investigate the character of the interstrip region after type inversion, the interstrip I–V curves were measured. In Fig. 17 I–V curves measured with floating detector backplane are presented. The non-linear shape of the curves shows clearly that the connection between the strips is not ohmic and indicates a structure consisting of two diodes, connected back to back.

The DC interstrip resistance was evaluated from the I–V measurements for different bias voltages in the detector. As it is shown in Fig. 18, for low bias voltages the DC interstrip resistance increases slowly with increasing bias voltage and rises when the bias approaches the depletion voltage. The minimum resistance obtained for the lowest bias voltages was of the order of 1 MΩ. In Fig. 19 the AC interstrip resistance as a function of bias voltage is shown. For low frequencies (< 10 kHz) the AC resistance approaches the value derived from DC measurements. At higher frequencies it is lower but still high enough to assure good strip isolation, even before full depletion.

4.4. p + side after inversion

We investigated the region near the p + strips by means of radiation with specific absorption range. We measured the counting rate vs. the detector bias voltage, either shining on the p + side the light of an infrared diode or irradiating with α particles from an ^{241}Am source. In both cases the characteristic length of radiation in silicon was of the order of 10 μm, although the depth profile of the ionisation was very different. For the americium source first we performed a threshold scan in order to identify the 60 keV X-ray peak and to cross-check the preamplifier gain. Afterwards we set the threshold at ~ 1.5 MIP in order to reject the X-rays. Because of the low intensity of the ^{241}Am source, for the α we summed the number of counts over a group of strips. In Figs. 20 and 21 the number of counts vs. bias voltage is shown

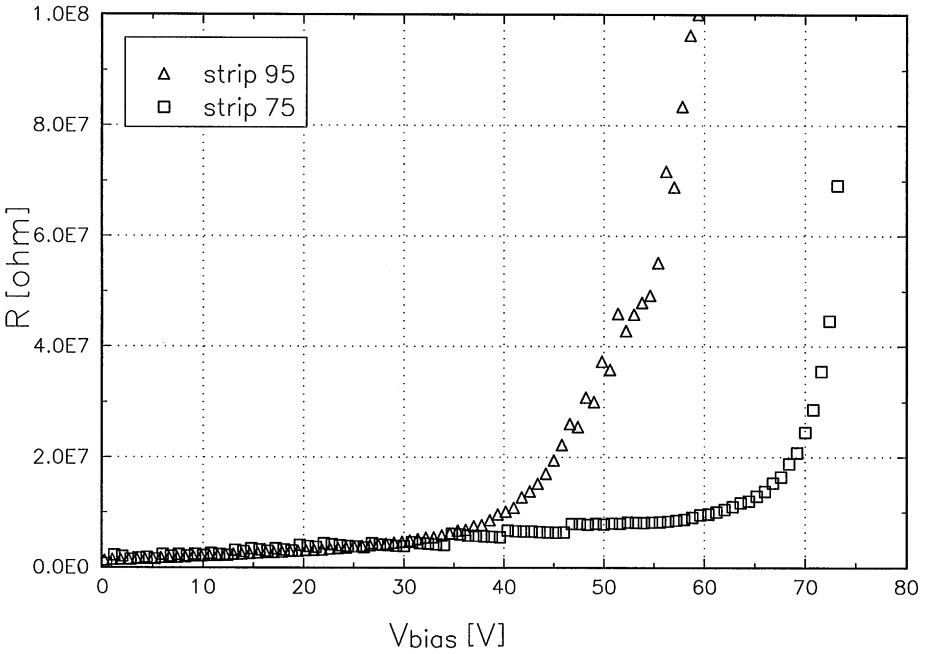

Fig. 18. DC interstrip resistance obtained from I–V measurements vs. detector bias voltage. Depletion voltages for strips 75 and 95 are 90 and 60 V, respectively.

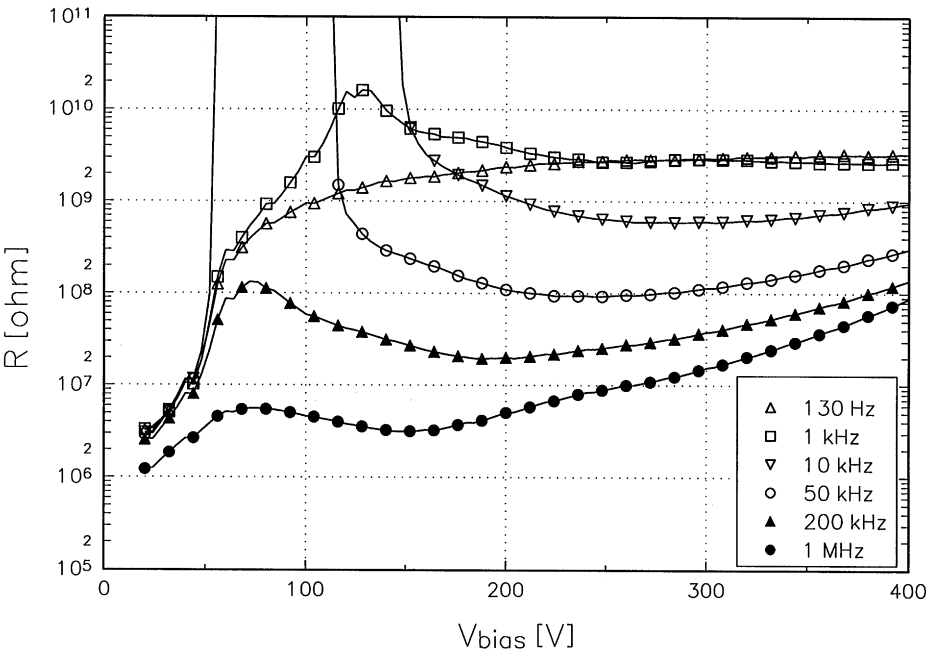

Fig. 19. Interstrip resistance obtained from AC measurements for strip 95.

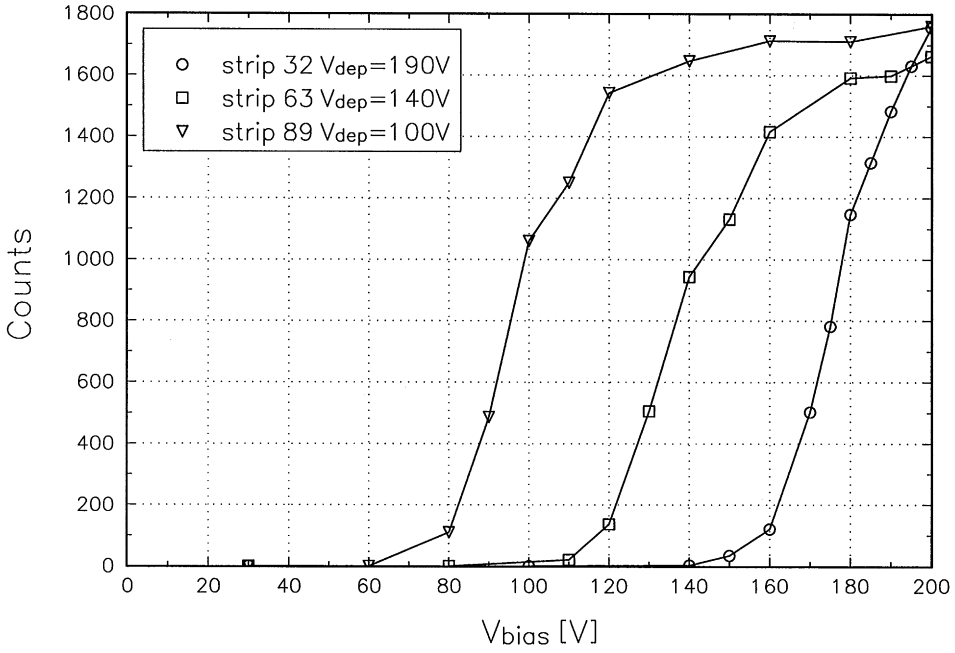

Fig. 20. Number of counts vs. bias voltage obtained with infrared diode.

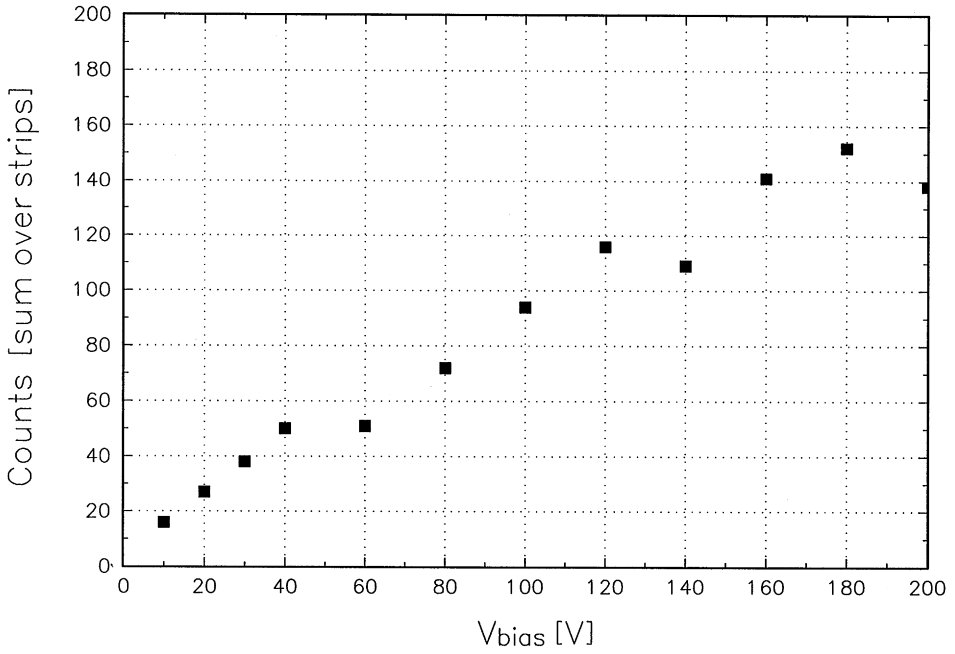

Fig. 21. Number of counts vs. bias voltage obtained with α source, summed for strips from 33 ($V_{dep} = 180$ V) to 93 ($V_{dep} = 100$).

respectively for the infrared diode and for the ^{241}Am source. For the diode there are no counts for bias voltages below the respective depletion voltage of each strip while for the α there are counts even for the lowest applied voltages, which are much lower then the depletion voltages for all strips in the group. The infrared light does not penetrate the metal electrodes which cover and overlap the p + implants. The comparison of data from the diode light and the α's could indicate that there is always a thin junction layer underneath the p + implants, i.e. in the region where the α's deposit charge while infrared light does not. Results leading to similar conclusions were reported in Ref. [8].

5. Conclusions

The silicon strip detectors employed in the NA50 experiment provide us with an experimental evidence that standard *p-on-n* detectors work well after type inversion. There are three main factors supporting this conclusion, namely that a good detector efficiency is preserved, that no detector breakdown is observed and that there is a good isolation between the p + strips.

The HV scan appears to be a powerful tool in monitoring depletion voltages so that the bias voltage can be adjusted during the data taking period.

Concerning the physical behaviour of the detector we found that in order to remove the electron surface layer from the interstrip region and therefore to recover the purely geometrical value of detector capacitancies one needs to bias the detector with a voltage much higher than the depletion one. The measurements show that for a limited range of oscillator frequencies one can still use the C–V method to estimate the depletion voltage of inverted detectors. The performed measurements suggest the existence of a junction underneath the p + implant. The observed frequency dependence of the radiation effects points to a complex system of electrically active defects.

References

[1] B. Alessandro et al., Nucl. Instr. and Meth. A 409 (1998) 167.
[2] ATLAS Inner Tracker Technical Design Report, vol. 2, CERN/LHCC/97-17, p. 394.
[3] B. Allesandro et al., Nucl. Instr. and Meth. A 419 (1998) 556.
[4] L. Dezille et al., Nucl. Instr. and Meth. A 386 (1997) 162.
[5] L. Andricek et al., ATLAS Internal Note INDET-NO-191, 10 November 1997.
[6] E. Fretwurst et al., Nucl. Instr. and Meth. A 342 (1994) 119.
[7] W. Dabrowski, K. Korbel, Nucl. Instr. and Meth. A 276 (1989) 270.
[8] L.J. Beattie et al., ATLAS Internal Note INDET-NO-194, 9 December 1997.